Industrial and Engineering Chemistry Research, Volume 59, Issue 36, September 2020, pp. 16068-16076
DOI:10.1021/acs.iecr.0c02387

Lanthanide doped MIP nano-architecture for the detection of melatonin

Erdoğan Özgür, Hirak K. Patra, Anthony P. F. Turner, Adil Denizli, Lokman Uzun

Abstract

Polymerisable terbium(III) complex-based fluorescent molecular imprinted smart nanoparticles were synthesised for the quantitative determination of potential metabolic destitution biomarkers. Melatonin has been reported to one of the key factors in Seasonal Affective Disorder (SAD) and was chosen as a model metabolite to demonstrate a novel MIP nanoparticle sensor. We exploited lanthanide ion complexes in our biosensing platforms due to their deeper penetration ability, negligible auto-fluorescence, lack of photo bleaching and photo blinking, and their sharp absorption and emission lines, long lifetime and extreme photo stability. Given the high affinity of lanthanide ions for carboxylic acid groups, we used two amino acid-based functional monomers, N-methacryloyl-L-aspartic acid (MA-Asp) and N-methacryloyl-L-tryptophan (MA-Trp), to coordinate terbium(III) ions and melatonin, respectively. The fluorescent MIP nanoparticles were synthesised using a miniemulsion polymerisation technique after forming complexes between terbium(III):MA-Asp and melatonin:MATrp molecules. Due to the polymerisability of lanthanide complexes, they were readily inserted into the polymeric chain, which enabled Professor homogeneous distribution as well as closer orientation to the imprinted cavities for selective melatonin recognition.

Keywords: Lantanite ions, molecular imprinting, fluorescent molecular imprinted nanoparticles.

Authors:
E. Özgür
Advanced Technologies Application and Research Center, Hacettepe University, Ankara, Turkey
Department of Chemistry, Faculty of Science, Hacettepe University, Ankara, Turkey

L. Uzun, A.Denizli
Department of Chemistry, Faculty of Science, Hacettepe University, Ankara, Turkey

H.K. Patra
Department of Clinical and Experimental Medicine, Linkoping University, Linkoping, Sweden
Department of Chemical Engineering and Biotechnology, University of Cambridge, Cambridge, UK

A.P.F. Turner
Professor Emeritus, SATM, Cranfield University, Bedfordshire, UK

Introduction

Lanthanide based luminescent nanoparticles (NPs) are promising alternative to fluorescent quantum dots (QDs) and organic dyes **(Wang et al. 2015)**. The weak photostability (photobleaching in a few minutes on exposure to light), low quantum yield, narrow excitation bands, broad emission bands, small Stokes shifts and relatively short lifetime of 1-5 s **(Forrest et al. 2011)** have limited the biological application of traditional organic dyes. QDs are also known as semiconductor nanocrystals and endow unique optical properties such as better chemical stability, a broad excitation range, a narrow emission peak, ultra high brightness and resistance to photobleaching, and thus overcome some of the deficiencies of organic dyes **(Duan et al.,2014).** However, potential toxicity due to the presence of heavy metal ions in their structure (CdSe, CdS) **(Parak et al. 2005)**, solubility in aqueous and biologically environments and complicated bio-functionalisation strategies have also limited their use in biological applications as fluorescent probes **(El-Sayed et al. 2005; Nie et al. 2005; Duan et al. 2014).** These drawbacks of organic dyes and QDs have led the researchers to investigate novel compounds such as lanthanide ions. Lanthanide ions (Ln^{3+}) possesl long luminescence lifetimes (~1 ms), which enables time resolved detection (**Härmä et al. 2011**), due to the formally forbidden 4f–4f electronic transitions, compared to organic dyes. The emission wavelengths of lanthanides also alter over a small range, because the 4f orbitals do not directly contribute to chemical bonding due to the shielding effect of the 5s and 5p orbitals, so the energy level of these orbitals are not affected by the surrounding environment (or matrix) and nanoparticle size **(Bouzigues et al. 2011; Meade et al. 2014)**. Hence, the absorption bands (1-5 nm broad), narrow emission bands (10 nm broad) and large effective Stokes shifts (~150 nm for YVO_4:Eu nanoparticles) **(Alexandrou et al. 2004)** of lanthanide ions attract considerable interest in their use as luminescence probes and labels for applications in imaging and sensing **(Haase et al. 1999; Boilot et al. 2000; Wang et al., 2008; Bouzigues et al. 2011)**. Lanthanide ions of europium (III) and terbium (III) in particular, have been widely investigated for biosensing and imaging in analytical/bioanalytical applications **(Schäferling, 2012; Wang et al. 2015).**

The combination of lanthanide ions (or their complexes) and nanoparticles to create novel hybrid nanomaterials has received much attention in research fields such as sensing, biomedical imaging and drug delivery etc. **(Gunnlaugsson et al. 2014)**. Incorporation of lanthanide ions into molecularly imprinted polymeric materials can provide specific binding events for many biomedical and diagnostic analyses due to their excellent chemical and optical properties (**Härmä et al. 2001**; **Wang et al. 2015**). Such multifunctional nanostructures offering molecular imprinting for specific biorecognition with fluorescent emission have been consider as a new class of researcher in the last years **(Qin et al. 2011; Jang et al. 2011; Labhasetwar et al. 2010).**

Molecular imprinting mimics the specific biorecognition ability of biological systems by using polymeric structures with similar interactions **(Whitcombe et al. 2014; Schirhagl, 2014).** Molecularly imprinted polymeric materials are generally produced by bulk polymerisation, but disadvantages such as the relatively low number of binding sites near the surface, heterogeneity in binding affinity, low rebinding capacity and slow rebinding kinetics limit their application in molecular diagnostics at the nanoscale **(Ding and Heiden, 2014; Martin-Estaban et al. 2010, Ye and Haupt, 2004).** So, nanoparticles with their high surface area to volume ratio, high binding afinity and capacity, and relatively high mass transfer due the binding sites being on or near the surface compared with traditional molecularly imprinted materials, have attracted attention for molecular recognation at the nanoscale (**Ding and Heiden, 2014**). Molecularly imprinted luminescent nanocomposites can be produced by using

fluorescent monomers during the synthesis process of molecularly imprinted polymers **(Powell et al. 1998)**, copolymerisation of luminescent nanomaterials, such as QDs, lanthanide doped NPs, fluorescent dyes with functional groups, cross linkers and target molecules (synthesis of molecularly imprinted polymers occurs by the copolymerisation of functional monomers and cross-linkers in the presence of the target) **(Li et al. 2013)** and encapsulation strategies **(Wang et al. 2012).**

Briefly, polymerisable terbium(III) complex-based fluorescent MIP nanoparticles have been synthesised for the quantitative determination of potential metabolic biomarkers. The melatonin molecule has been chosen as a model metabolite to demonstrate this MIP nanoparticle sensor. Melatonin is part of the metabolic pathway of L-tryptophan and has been reported to one of the key factors in seasonal affective disorder (SAD) **(Peiser, B. 2009).** Melatonin can be determined by high-performance liquid chromatography with fluorescence, mass spectrometry, gas chromatography and mass spectrometry, radioimmunoassay, enzyme-linked immunosorbent assay, electrochemical detection and immunoprecipitation. However, there is an unmet need for a simple, inexpensive sensor-based system for use in point-of-care applications. Herein, we have exploited lanthanide ion complexes in our biosensing platforms due to their deeper penetration ability, negligible auto-fluorescence, lack of photo bleaching and photo blinking, and their sharp absorption and emission bands, long lifetime and extreme photo stability. It is known that carboxyl groups of amino acids serving as chelates are particularly suitable ligands with high affinity **(Otting et al. 2004).** Chelating agent can prevent the release of free lanthanides into the working area and protect the lanthanide from vibrational energy dissipation by oscillators like -OH of water **(Kielar et al. 2007; Butler and Parker, 2013).** Two amino acid-based polymerisable functional monomers, N-methacryloyl-L-aspartic acid (MAAsp) and N-methacryloyl-L-tryptophan (MATrp) **(Fig. S1) (Hür et al. 2007)** were synthesised to coordinate terbium(III) ions and melatonin, respectively. The fluorescent MIP nanoparticles were synthesised using micro-emulsion polymerisation techniques after forming complexes between terbium(III):MAAsp and melatonin:MATrp molecules. Due to the polymerisability of lanthanide complexes, they were readily inserted into the polymeric chain, which enabled homogeneous distribution as well as closer orientation to the imprinted cavities for selective melatonin recognition. By this approach, we aimed to developed an alternative nanoparticle-based sensor system that has promising advantages to commercially available melatonin detection method.

2. Experimental

2.1. Materials

L-tryptophan, L-aspartic acid, terbium(III) nitrate pentahydrate, poly(vinyl alcohol) (PVA), 2-hydroxyethyl methacrylate (98%) (HEMA), ethylene glycol dimethacrylate (EGDMA), α,α'-azoisobutyronitrile (AIBN), 1H-benzotriazole, triethylamine (≥99.5%), methacryloyl chloride (≥97%), sodium dodecyl sulfate (SDS), ammonium persulfate, sodium bicarbonate, sodium bisulfite, melatonin and serotonin hydrochloride were were supplied by Sigma Chemical Co. (St. Louis, USA). All HPLC grade solvents were from commercial sources and used without further purification. All other chemicals used were reagent grade from Merck A.G. (Darmstadt, Germany) unless otherwise noted. Laboratory glasswares were kept overnight in a nitric acid solution of 4M. All water used during the experiments was purified using a Barnstead (Dubuque, IA, USA) ROpure LP®reverse osmosis unit.

2.2. Synthesis of Fluorescent Tb(III)MAAsp$_3$ Complex

The fluorescent complex was prepared using Tb(III) and N-methacryloyl-L-aspartic acid (MAAsp), in 1:3 molar ratio as [Tb(III):MAAsp]. In brief,, MAAsp (3 mmol) and ammonium oxalate monohydrate (0.5 mmol), (0.5 mmol, 71 mg) were dissolved in 20 mL of deionized water (DI). The pH was adjusted between 6.0-7.0 for the complexation, by dropwise addition of NaOH (1.0 M). Followed by slowly addition 1 mmol of $Tb(NO_3)_3.5H_2O$ into the previous solution.. The mixture was magnetically stirred at 150 rpm for 24 h, then, the white precipitate, the crystals of the complex, was harvested from filtrate solution. The characterisation of the fluorescent complex was performed by spectrofluorimetric measurements (Shimadzu, RF 5301, Tokyo, Japan).

2.3. Synthesis of Molecularly Imprinted Fluorescent Nanoparticles

Melatonin imprinted fluorescent nanoparticles were synthesised by two-phase miniemulsion polymerisation. Prior to polymerisation, the aqueous phase 1 was prepared by dissolving of PVA (93 mg), SDS (15 mg) and sodium bicarbonate (12.5 mg) in 5 mL of DI. The aqueous phase 2 was prepared by dissolving of PVA (50 mg) and SDS (50 mg) in 100 mL of DI. The organic phase 3 was formed by mixing the functional N-methacryloyl-L-tryptophan (MATrp, 0.125 mmol), 2-hydroxyethyl methacrylate (HEMA, 0.5 mmol) and crosslinker, ethylene glycol dimethacrylate (EDMA, 15 mmol). The solution in organic phase was slowly added to the aqueous phase 1. In order to obtain miniemulsion, the mixture was homogenised at 25000 rpm by a homogenizer. Then, template molecule (melatonin) (0.125 mmol) was added to the miniemulsion and mixed using a magnetic stirrer for 30 min for effective functional monomer-template interaction. During this process, polymerisable lanthanide complex (0.125 mmol) was added into the miniemulsion medium. After homogenisation, the mixture was slowly added to the aqueous phase 2 in a sealed-cylindrical polymerisation reactor, while dissolved oxygen was removed by nitrogen gas through the mixture for 5 min. The reactor was magnetically stirred at 300 rpm. The polymerisation mixture was slowly heated to 40°C. Then, initiators, sodium bisulfite (57.5 mg) and ammonium persulfate (63 mg), were added into the solution. Polymerisation was continued at 40°C for 24 h. The particles in larger size were removed by centrifuging at 5000 rpm. The melatonin imprinted fluorescent nanoparticles were washed with DI and DI /ethyl alcohol mixtures, in order to remove unreacted monomers, surfactant and initiator. For each washing step, the solution was centrifuged at 60000 rpm for 30 min (Allegra-64R Beckman Coulter, USA); then, the nanoparticles were dispersed in fresh washing solution. After last washing step, the melatonin imprinted fluorescent nanoparticles were dispersed in DI containing 0.3% sodium azide and stored at 4°C. The non-imprinted fluorescent nanoparticles were also synthesised using the same polymerisation method in the absence of melatonin and N-methacryloyl-L-tryptophan (MATrp), respectively, to provide controls.

>>>Scheme 1<<<<

3. Results and Discussion

3.1. Characterisation of N-Methacryloyl L-Tryptophan and N-Methacryloyl L-Aspartic Acid Monomers

The FTIR-ATR spectrum of MATrp is shown in **Fig. S1**. The characteristic 3398 cm^{-1} absorption band was due to (secondary amine group) N-H stretching. Absorption bands at 3075-3015 cm^{-1} belong to aromatic C-H stretching. C-H stretching band of alkyl group is at 2972 cm^{-1}. C=O stretching band of acid is observed at 1657 cm^{-1}, and

C=C stretching band is at 1577 cm^{-1}. C-N stretching aromatic band is at 1488 cm^{-1}. Absorption bands at 740-770 cm^{-1} belong to aromatic C-H bending **(Larkin, 2011)**.

The FTIR-ATR spectrum of MAAsp showed a characteristic carbonyl band at 1567 cm^{-1}, and the 3395 cm^{-1} absorption band was due to (secondary amine group) N-H stretching. The C-N symmetric and asymmetric stretching bands were observed at 1010 cm^{-1} and 1388 cm^{-1} as shown in **Fig. S1 (Larkin, 2011)**. The FTIR-ATR spectrum shows that MATrp and MAAsp were synthesised successfully.

3.2. Characterisation of Fluorescent Tb(III)-MAAsp$_3$ Complex

Tb(III)-MAAsp$_3$ complex has four classical fluorescent emission bands (**Fig. 1)** at 547 nm ($^5D_0$-$^7F_0$ transition), 586 nm ($^5D_0$-$^7F_1$ transition), 622 nm ($^5D_0$-$^7F_3$ transition), and 763 nm ($5D_0$-$^7F_4$ transition), respectively. These four classical fluorescent emission bands show that Tb (III) ions were successfully incorporated into the complex structure and the interaction between ligand (MAAsp) and ion (Tb(III)) were strongly formed.

>>>Fig. 1<<<

3.3. Characterisation of Molecularly Imprinted Fluorescent Nanoparticles

The surface properties and depth of the melatonin imprinted fluorescent nanoparticles were determined by AFM. AFM measuments were performed with AFM (Nanomagnetics Instruments, Oxford, UK) in dynamic mode and under an air atmosphere. Nanomagnetics' AFM system makes measurement at high resolution (i.e., 4096x4096 pixels). Experimental parameters were oscillation frequency (341.30 Hz), vibration amplitude (1 V_{RMS}) and free vibration amplitude (2 V_{RMS}). Samples were scanned with a 2 µm/s scanning rate and 256x256 pixels resolution to obtain a view of a 1 µm × 1 µm area. The imprinted fluorescent nanoparticles had a spherical shape and their measured size was around 70 nm **(Fig. 2a).**

The particle size and the distribution of the nanoparticles were determined using a Zetasizer (NanoS, Malvern Instruments, London, UK). During measurements, the light scattering was at incidence angle 90° and 25°C. For data analysis, density and refraction index of DI were used as 0.88 mPa s^{-1} and 1.33, respectively and the data was counted as nanoparticles per second. The size of the melatonin imprinted and non-imprinted nanoparticles are shown in **Fig. 2b-c.** The Z-Average hydrodynamic diameter of melatonin imprinted nanoparticles was found to be 63.27 nm with a narrow polydispersity index as 0.093. The Z-Average of melatonin non-imprinted nanoparticles was 73.80 nm with a higher polydispersity index of 0.381 compared to imprinted particles. These results show that the polymerisation technique is appropriate for the synthesis of imprinted nanoparticles with the desired features.

>>>Fig. 2<<<

3.4. Detection of melatonin using melatonin-imprinted fluorescent nanoparticles

3.4.1. Effect of Template (Melatonin) Concentration

In order to optimise melatonin detection, the imprinted fluorescent nanoparticles were examined for melatonin adsorption from aqueous solutions. The most effective pH, melatonin concentration, ionic strength (sodium chloride (NaCl) concentration), time and temperature were determined to be in the ranges of 4.0 - 8.0, 0.01 ng/mL-0.5 ng/mL, 0.1 M - 1.0 M, 15 min - 180 min and 4ºC - 40ºC, respectively. Continuous agitation at 50 rpm using rotator was maintained during the interaction of the fluorescent nanoparticles with aqueous melatonin soltuion while varying the conditions given above.

The melatonin imprinted fluorescent nanoparticles delivered two different linear regions for the detection of melatonin **(Fig. 3).** The results dsuggest that melatonin bound to the melatonin imprinted fluorescent nanoparticles through two different orientations with high affinity. Melatonin imprinted fluorescent nanoparticles showed a linearity of 99% in the concentration range of 0.01 ng/mL - 0.05 ng/mL and a linearity of 97% in the concentration range of 0.05 ng/mL - 0.5 ng/mL. When the results were plotted as intensity vs log(concentration), only a single linear working range were clearly obeserved with a regression coefficient of 96% (Fig. 3b, inset). According to the equation, the limit of detection and the limit of quantification values were calculated as 0.121 and 0.411 pg/mL, respectively.

>>>Fig. 3<<<

In general, the control of melatonin synthesis and secretion, and its synchronisation with the 24-hour body clock are dominated by the light/dark cycle. Endogenous serum melatonin concentration in healthy young adults is in the range of 10 pg/mL typically during daylight hours and at night about 40 pg/mL (Pandi-Perumal, 2007). Hence, melatonin-imprinted fluorescent nanoparticles can be used for the detection of melatonin over the normal range from 10 to 40 pg/mL and the melatonin value in SAD patients, which reaches about 60 pg/mL and where the secretion is longer in winter than in summer (Checkley, 1993; Wehr, 2001).

3.4.2. Evaluation of the Effects of pH, Ionic Strength, Time, and Temperature

The effect of pH on the adsorption capacity was estimated using different buffer systems with pH ranging from 4.0 - 8.0. The optimal pH was determined as pH 5.0 **(Fig. 4a).** At lower and higher pH values, the adsorption capability of the nanoparticles was significantly decreased. The plausible explanation is that the ligand (tryptophan-based functional monomer, MATrp) is uncharged at pH 5.0 and therefore the hydrophobic interactions at this pH are more selective and via hydrophobic interactions, can achieve higher adsorption capabilities. This is related to structural characteristics of the functional monomer which was used, because molecularly imprinted nanoparticles were synthesised via hydrophobic interactions. A polymerisable derivative of tryptophan, a hydrophobic amino acid, was used for the coordination of melatonin.

The optimum ionic strength was estimated using NaCl with concentration range between 0.1 M - 1.0 M. The ionic strength of the neutral salt added to the medium affects the solubility of the analyte molecules. Ionic strength is determined by the charge and the concentration of cations and anions that form the salt. With increasing concentration of salt there is a decrease in the adsorption of melatonin (**Fig. 4b).** This is because of increasing salt

concentration melatonin loose the solubility and the interaction between melatonin and nanoparticles increased. The adsorption process reached to the equilibrium value almost in 60 minutes (**Fig. 4c).** After this point, the change of adsorption is not significant. This result implies that the adsorption kinetics of fluorescent nanoparticles is relatively rapid. The effect of temperature on the adsorption capacity was determined over different temperatures ranging from 4°C - 40°C **(Fig. 4d).** TAn increase in temperature resulted a significant increase in melatonin adsorption capabilities. These results also imply that the interactions between melatonin and melatonin imprinted fluorescent nanoparticles have a basically hydrophobic character. Hydrophobic interactions depend on the change in the entropy of space and the possibility of hydrophobic interactions between analyte and nanoparticles is enhanced with increasing in the entropy (**Denizli et al. 2005).**

>>>Fig. 4<<<

3.5. Determination of Imprinting Selectivity

To show the selectivity of melatonin imprinted fluorescent nanoparticles, the competitive adsorption of melatonin, serotonin and tryptophan molecules were investigated. Melatonin biosynthesis involves four enzymatic steps from the essential dietary amino acid tryptophan, which follows a serotonin pathway. As seen in **Fig. 5a**, imprinted fluorescent nanoparticles did not give any significant response to serotonin and tryptophan molecules. Additionally, non-imprinted nanoparticles were synthesised for control purpose. The non-imprinted nanoparticles interacted with analyte molecules, but non-imprinted fluorescent nanoparticles did not give any significant response to analyte molecules (melatonin, serotonin and tryptophan) (**Fig. 5b).**

>>>Fig. 5<<<

Analyte solutions with same concentration of 0.03 ng/mL were allowed to interact with melatonin imprinted fluorescent nanoparticles and also with non-imprinted fluorescent nanoparticles. Changes in fluorescence emission intensity of nanoparticles were measured before and after adsorption. Then, these results were normalised to see the changes in emission intensity. By using these data, we also analysed the selectivity of the imprinted nanoparticles. The distribution constants (k_D), selectivity (k) and the relative selectivity constants (k') were calculated and given in **Table. 1**. The following equations were used to calculate these parameters:

$k_{D,analyte}$ = Intensity*/ Intensity ^{0}

$k_{melatonin} = k_{D,melatonin} / k_{D,competitive}$

$k' = k_{MIP} / k_{NIP}$

$k_{D,analyte}$ is the distribution constant of the target metabolite; intensity* is the normalised intensity of target metabolite (intensity*= intensity^0 - Intensity^{analyte}); intensity^0 is emission the intensity of fluorescent nanoparticles (without interaction with any analyte); $k_{melatonin}$ is the selectivity of fluorescent nanoparticles for melatonin against the competitive metabolites and k' is the relative selectivity constants of fluorescent imprinted nanoparticles against fluorescent non-imprinted nanoparticles.

As shown in **Table 1**, the changes in emission intensity of fluorescent imprinted nanoparticles are significant. The selectivity constants for melatonin molecules determined as 14.97 and 15.63 against serotonin and tryptophan, respectively. These values for non-imprinted fluorescent nanoparticles were also calculated as 0.8175 and 0.6344, respectively. The relative selectivity constants (k') for melatonin molecules, which illustrate imprinting efficiency, were calculated as 18.31 and 24.64 in respect of the competitor molecules, serotonin and tryptophan, respectively. The results show that melatonin imprinted fluorescent nanoparticles have selective recognition ability against serotonin and tryptophan with a selectivity of 18.31 and 26.64, respectively. As a conclusion, melatonin imprinted fluorescent nanoparticles could be used in terms of analytical performance and selectivity parameters for the detection of seasonal affective disorder.

Table 1. Selectivity and parameters for MIP nanoparticles.

	MIP			NIP			
	Intensity*, mAU	k_D	k	Intensity*, mAU	k_D	k	k'
Melatonin	621.3	0.8965		66.3	0.1714		
Serotonin	41.5	0.0599	14.97	81.2	0.2097	0.8175	18.31
Tryptophan	39.8	0.0574	15.63	104.6	0.2702	0.6344	24.64

*: Normalised values of intensity. Normalised values are the difference in the fluorescence intensity of fluorescent nanoparticles before and after adsorption.

The intensity of MIP before adsorption: 693 mAU and the intensity of NIP before adsorption 387 mAU.

4. Conclusions

SAD (winter depression) is characterised by recurrent depressive symptoms during the short photoperiod. The active secretion of melatonin is longer in winter than in summer in patients with SAD (winter depression) due to the lack of sunlight. Changes in of melatonin secretion during this period were have been hypothesised to play a role in the pathogenesis of SAD and prompted its treatment with phototherapy. In order to provide for the possibility of developing a stable point-of-care test to accompany the therapy, we explored a novel sensing technology using fluorescent imprinted polymer nanoparticles. Efficient and selective fluorescent nanoparticles were obtained by directly inserting lanthanide ion complexes into molecularly imprinted polymeric chains. The fluorescent nanoparticles showed high affinity and selectivity against melatonin, which was 18.3-fold and 24.6-fold higher than that for serotonin and tryptophan. The strategy proposed in this study is a generic, smart and promising approach which in this case delivered LOD and LOQ values of 0.121 and 0.411 pg/mL. This provided a potential nanosensor with high selectivity, high specificity to the target molecules and quite low detection/quantification limits for melatonin, which could be used for melatonin monitoring during the winter period of SAD.

References

1- Dengfeng P, Qiang J, Xian C, Ronghua M, Bing C, Gongxun B, Jianhua H, Xvsheng Q, Xianping F, Feng W (2015) Lanthanide-doped energy cascade nanoparticles: full spectrum emission by single wavelength excitation. Chem Mater 27: 3115-3120.

2. Nune SK, Gunda P, Majeti BK, Thallapally PK, Forrest ML (2011) Advances in lymphatic ımaging and drug delivery. Adv Drug Delivery Rev 63: 876-885.

3- Burda C, Chen XB, Narayanan R, El-Sayed MA (2005) Chemistry and properties of nanocrystals of different shapes. Chem Rev 105: 1025-1102.

4- Yao J, Yang M, Duan Y (2014) Chemistry, biology, and medicine of fluorescent nanomaterials and related systems: new ınsights into biosensing, bioimaging, genomics, diagnostics, and therapy. Chem Rev 114: 6130-6178.

5- Gao XH, Yang LL, Petros JA, Marshal FF, Simons JW, Nie SM (2005) In vivo molecular and cellular imaging with quantum dots. Curr Opin Biotechnol. 16: 63-72.

6- Kirchner C, Lied T, Kudera S, Pellegrino T, Muñoz Javier A, Gaub HE, Stölzle S, Fertig N, Parak WJ (2005) Cytotoxicity of colloidal CdSe and CdSe/ZnS nanoparticles. Nano Lett 5: 331-338.

7- Huignard A, Gacoin T, Boilot JP (2000) Synthesis and properties of colloidal YVO_4:Eu phosphors. Chem Mater. 12: 1090-1094.

8- Meyssamy H, Riwotzki K, Kornowski A, Naused S, Haase M (1999) Wet-chemical synthesis of doped colloidal nanomaterials: particles and fibers of $LaPO_4$:Eu, $LaPO_4$: Ce, and $LaPO_4$:Ce,Tb. Adv Mater 11: 840-844.

9- Wang L, Li P, Wang L (2008) Luminescent and hydrophilic LaF_3-polymer nanocomposite for DNA detection. Luminescence 24: 39-44.

10- Heffern MC, Matosziuk LM, Meade TJ (2014) Lanthanide probes for bioresponsive imaging, Chem Rev 114: 4496-4539.

11- Bouzigues C, Gacoin T, Alexandrou A (2011) Biological applications of rare-earth based nanoparticles. ACS Nano 11: 8488-8505.

12- Schäferling M (2012) The art of fluorescence imaging with chemical sensors. Angew Chem Int Ed 51: 3532-3554.

13- Yingxin Ma, Y Xu, Wang S, Wang L (2015) Luminescent molecularly-imprinted polymer nanocomposites for sensitive detection. Trends Analyt Chem 67: 209-216.

14- Soukka T, Härmä H (2011) Lanthanide nanoparticules as photoluminescent reporters, in: Hänninen, P., Härmä, H. (Eds.), Lanthanide Luminescence: Photophysical, Analytical and Biological Aspects. Springer Ser. Fluoresc. pp. 89-114.

15- Härmä H, Soukka T, Lövgren T (2001) Europium nanoparticles and time-resolved fluorescence for ultrasensitive detection of prostate-specific antigen. Clin Chem 47: 561-568.

16- Schirhagl R (2014) Bioapplications for molecularly imprinted polymers. Anal Chem 86: 250-261.

17- Whitcombe MJ, Kirsch N, Nicholls IA (2014) Molecular imprinting science and technology: a survey of the literature for the years 2004–2011. J Mol Recognit 27: 297-401.

18- Turkewitsch P, Wabdelt B, Darling GD, Powell W (1998) Fluorescent functional recognition sites through molecular imprinting. A polymer-based fluorescent chemosensor for aqueous cAMP. Anal Chem 70: 2025-2030.

19- Li DY, He XW, Chen Y, Li WY, Zhang YK (2013) Novel hybrid structure silica/CdTe/molecularly imprinted polymer: synthesis, specific recognition, and quantitative fluorescence detection of bovine hemoglobin. ACS Appl Mater Interfaces 5: 12609-12616.

20- Zhao YY, Ma YX, Li H, Wang LY (2012) Composite QDs@MIP nanospheres for specific recognition and direct fluorescent quantification of pesticides in aqueous media. Anal Chem 84: 386-395.

21- Comby S, Surender EM, Kotova O, Truman LK, Molloy JK, Gunnlaugsson T (2014) Lanthanide-functionalized nanoparticles as MRI and luminescent probes for sensing and/or imaging applications. Inorg Chem 53: 1867-1879.

22- Beaurepaire E, Buissette V, Sauviat MP, Giaume D, Lahlil K, Mercuri A, Casanova D, Huignard A, Martin JL, Gacoin T, Jean-Pierre Boilot JP, Alexandrou A (2004) Functionalized fluorescent oxide nanoparticles: artificial toxins for sodium channel targeting and ımaging at the single-molecule level. Nano Lett 4: 2079-2083.

23- Kielar F, Montgomery CP, New EJ, Parker D, Poole RA, Richardson SL, Stenson PA (2007) A mechanistic study of the dynamic quenching of the excited state of europium(III) and terbium(III) macrocyclic complexes by charge- or electron transfer. Org Biomol Chem 5: 2975-2982.

24- Butler SJ, Parker D (2013) Anion binding in water at lanthanide centres: from structure and selectivity to signalling and sensing. Chem Soc Rev 42: 1652-1666.

25-Su XC, Man B, Beeren S, Liang H, Simonsen S, Schmitz C, Huber T, Messerle BA, Otting G (2008) A Dipicolinic acid tag for rigid lanthanide tagging of proteins and paramagnetic NMR spectroscopy. J Am Chem Soc 130: 10486-10487.

26- Peiser B (2009) Seasonal affective disorder and exercise treatment: a review. Biol Rhythm Res 40: 85-97.

27- Hür D, Ekti SF, Say R (2007) N-Acylbenzotriazole mediated synthesis of some methacrylamido amino acids. Lett Org Chem 4: 585-587.

28- Di W, Ren X, Zhao H, Shirahata N, Sakka Y, Qin W (2011) Single-phased luminescent mesoporous nanoparticles for simultaneous cell imaging and anticancer drug delivery. Biomaterials 32: 7226-7233.

29- Oh WK., Jeong YS, Song J, Jang J (2011) Fluorescent europium-modified polymer nanoparticles for rapid and sensitive anthrax sensors. Biosens Bioelectron 29: 172-177.

30- Foy SP, Manthe RL, Foy ST, Dimitrijevic S, Krishnamurthy N, Labhasetwar V (2010) Optical imaging and magnetic field targeting of magnetic nanoparticles in tumors. ACS Nano 4: 5217-5224.

31- Larkin J (2011) Infrared and Raman Spectroscopy, Principles and Spectral Interpretation, Elsevier, Amsterdam, Netherland.

32- Öncel Ş, Uzun L, Garipcan B, Denizli A (2005) Synthesis of phenylalanine-containing hydrophobic beads for lysozyme adsorption. Ind Eng Chem Res 44: 7049-7056.

33- Ye L, Haupt K (2004) Molecularly imprinted polymers as antibody and receptor mimics for assays, sensors and drug discovery. Anal Bioanal Chem 378: 1887-1897.

34- Turiel E, Martin-Esteban A (2010) Molecularly imprinted polymers for sample preparation: A review. Anal Chim Acta 668: 87-99.

35- Ding X, Heiden PA (2014) Recent developments in molecularly imprinted nanoparticles by surface imprinting techniques. Macromol Mater Eng 299: 268-282.

36- Pandi-Perumal SR, Smits M, Spence W, Srinivasan V, Cardinali DP, Lowe AD, Kayumov L (2007) Dim light melatonin onset (DLMO): A tool for the analysis of circadian phase in human sleep and chronobiological disorders. Prog Neuropsychopharmacol Biol Psychiatry 31: 1-11.

37- Wehr TA, Duncan WC, Sher L, Aeschbach D, Schwartz PJ, Turner EH, Postolache TT, Rosenthal NE, (2001)A circadian signal of change of season in patients with seasonal affective disorders. Arch. Gen. Phychiatry 58: 1108-1114.

38- Checkley SA, Murphy DGM, Abbas M, Marks M, Winton F, Palazidou E, Murphy DM, Franey C, Binme C, Arendt J, Campos Costa D (1993) Melatonin Rhythms in Seasonal Affective Disorder. Br J Psychiatry 163: 332-337.

FIGURES

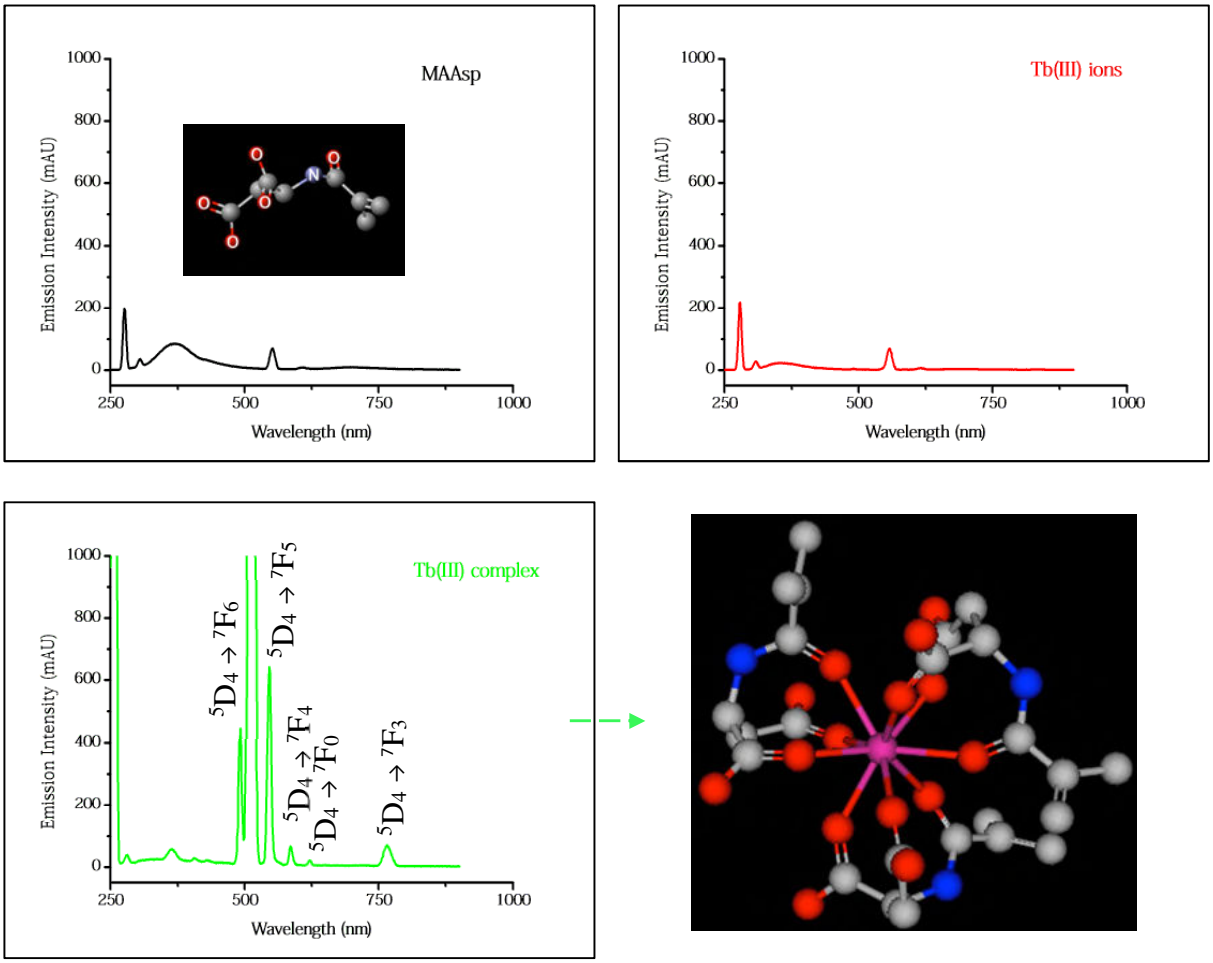

Fig. 1 Fluorescent emission spectra of Tb(III)-$MAAsp_3$ complex.

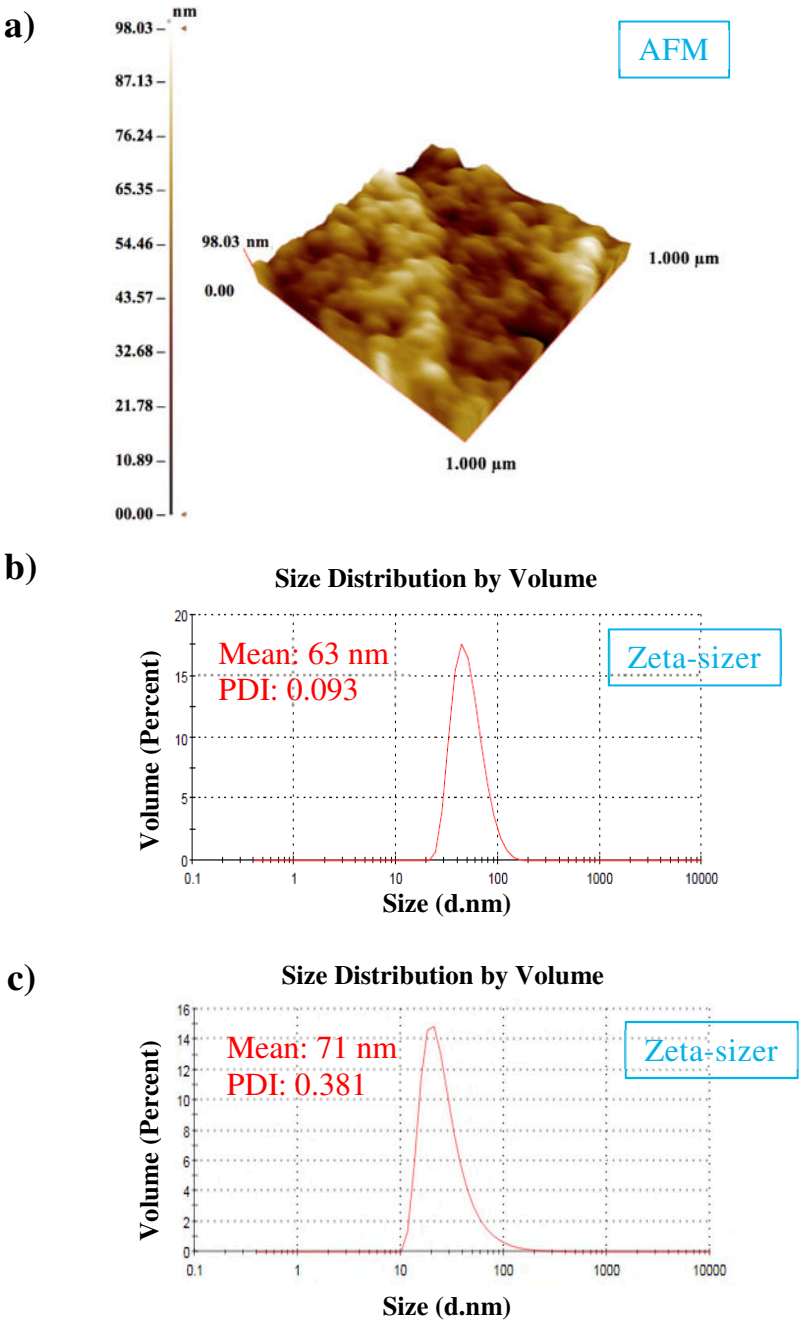

Fig. 2 a) 3-dimensional AFM image of imprinted fluorescent nanoparticles; **b)** hydrodynamic size (diameter) of melatonin imprinted nanoparticles and **c)** non-imprinted nanoparticles.

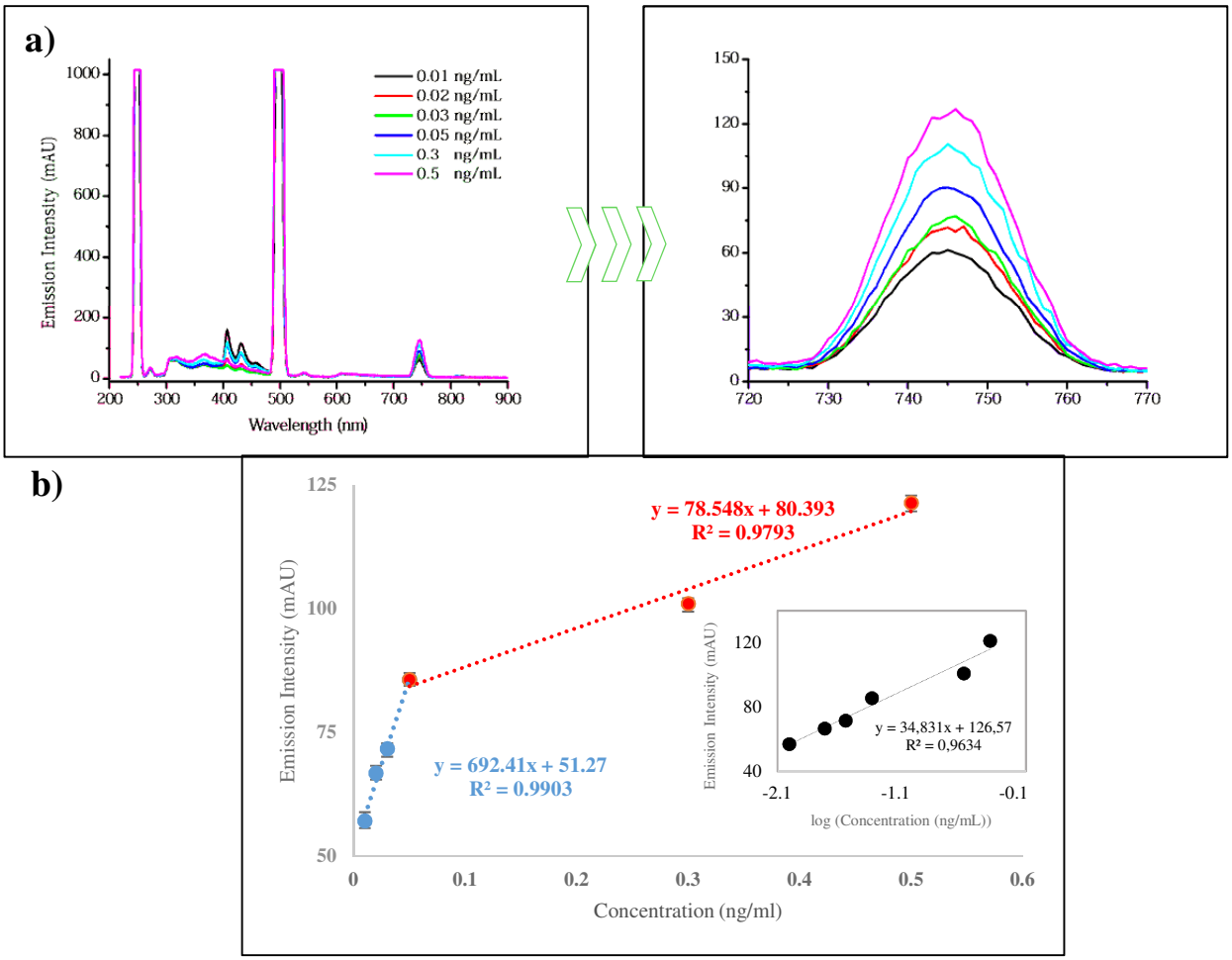

Fig. 3 a) Fluorescent emission spectra of melatonin adsorption process, **b**) correlation between concentration and emission intensity at 748 nm.

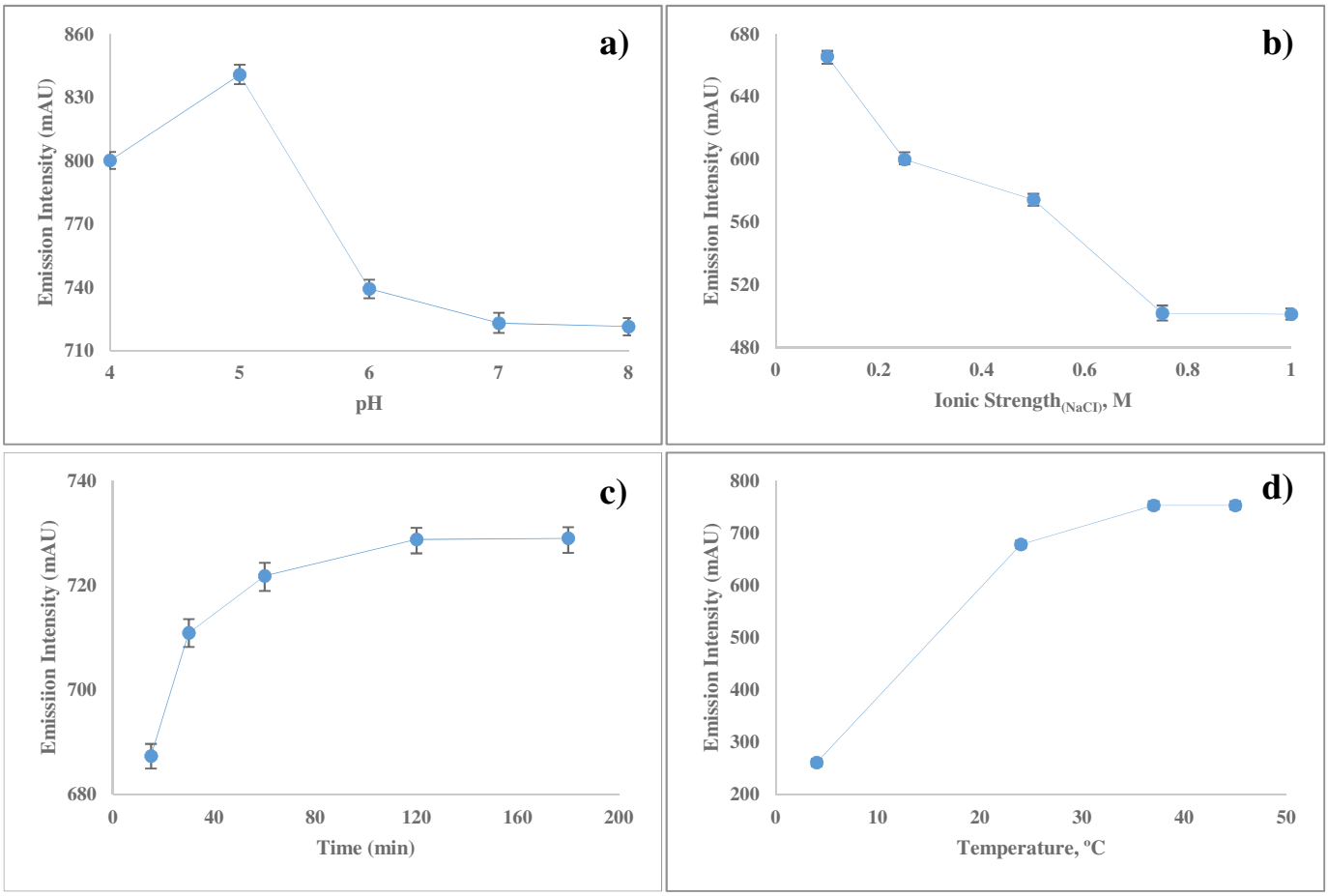

Fig. 4 a) Effect of pH (melatonin concentration of 0.03 ng/mL, emission values at 748 nm), **b)** Effect of ionic strength (melatonin concentration of 0.03 ng/mL, emission values at 748 nm), **c)** Effect of time (melatonin concentration of 0.03 ng/mL, emission values at 748 nm), **d)** Effect of temperature (melatonin concentration of 0.03 ng/mL, emission values at 748 nm).

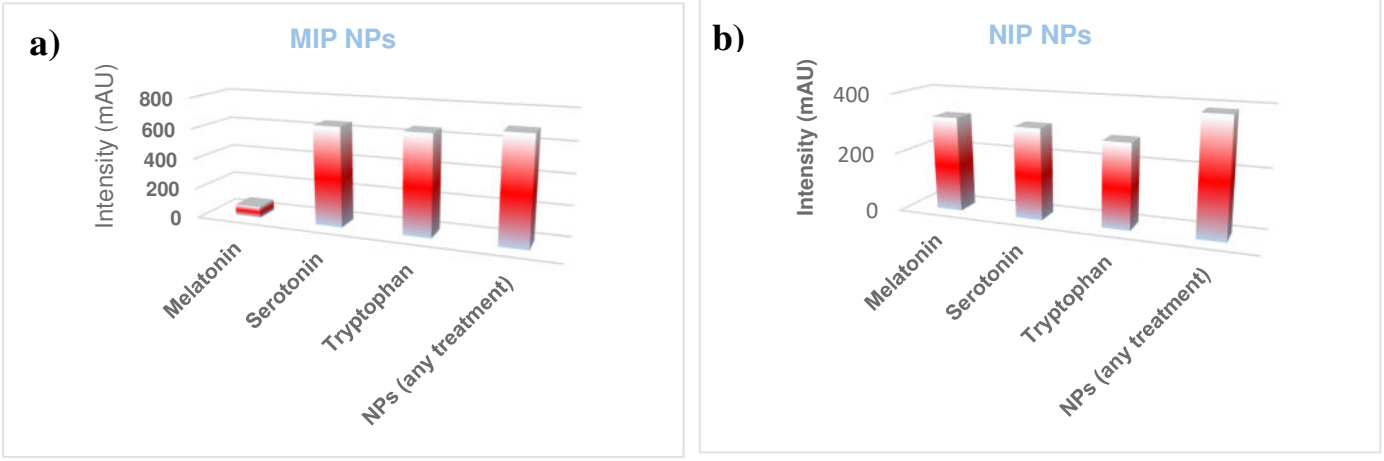

Fig. 5 Determination of selectivity. **a)** melatonin imprinted fluorescent nanoparticles, **b)** non-imprinted fluorescent nanoparticles (melatonin concentration of 0.03 ng/mL, emission values at 748 nm).

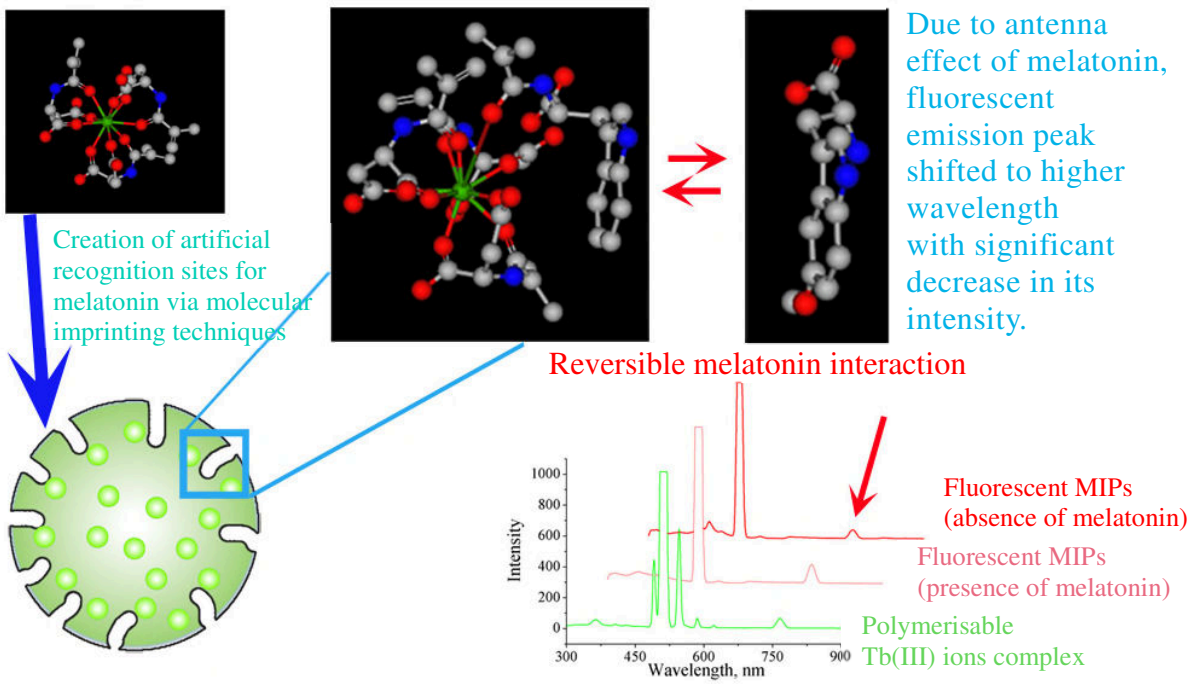

Scheme 1. Schematic illustration of Tb(III)-$(MAAsp)_3$ incorporated molecularly imprinted fluorescent NPs for spesific detection of melatonin.